A TWO-PHASE MODEL FOR SEDIMENT TRANSPORT IN RIVER FLOW

Massimo Greco[1], Michele Iervolino[2], Angelo Leopardi[3] & Andrea Vacca[2]

[1]Department of Hydraulic, Geotechnical and Environmental Engineering, University of Naples "Federico II", Italy
[2]Department of Civil Engineering, Second University of Naples, Italy
[3]Department of Civil and Mechanical Engineering, University of Cassino and Southern Lazio, Italy
E-mail: grecom@unina.it

Abstract

The paper introduces a 2D depth averaged model for the analysis of river morphodynamics, based on a two-phase formulation. Mass and momentum conservation principles are separately imposed for both phases. The model naturally accounts for unsteady non-equilibrium solid transport, since neither instantaneous adaptation hypothesis nor any *ad hoc* differential equation is employed to represent sediment dynamics. Results from numerical simulations for a 2D test-case are compared with literature experimental data and with available numerical solutions.

Introduction

The analysis of unsteady river flows requires adequate representation of several mutually interacting processes, such as the motion of the fluid and the erosion/deposition of solid particles. The most extensively used fluvial models have been built upon traditional hydraulics principles (Cao & Carling, 2002).

Indeed, Saint Venant - Exner equations are commonly used to predict the fluvial morphodynamics in depth-averaged either 1D or 2D approach. A standard approach suggests to evaluate sediment transport through an algebraic closure equation strictly valid for uniform flow conditions (e.g. Graf, 1998). The major drawback of this formulation comes from the validity of the instantaneous adaptation hypothesis, which is not satisfied whenever non-equilibrium transport conditions occur (Wu, 2007). Such an instance is often encountered in various fields of geomorphology and engineering, whenever rapid erosional transients are expected, such as valley forming floods (Brooks & Lawrence, 1999), sediment laden flows (Iverson, 1997; Takahashi, 1991), wave generated by dam break or overtop (Benoist, 1989), turbidity currents (Hu & Cao, 2009) and morphological changes induced by tsunamis (Simpson & Castelltort, 2006).

To overcome the above cited limitation, the Saint Venant - Exner formulation has been successively enriched by including an additional differential equation, describing the adaptation in time and in space of the actual value of the sediment discharge to the equilibrium value. To this aim, linear lag equations have been widely employed, along with proper expressions of the lag coefficient (e.g. Armanini & Di Silvio, 1988). Other dynamic equations, involving both temporal and spatial derivatives of the sediment discharge, were deduced either accounting for local inertia of sediment and shear induced by the flow in a simplified momentum balance (Di Cristo et Al., 2002; Parker, 1975), or describing the ensemble-averaged concentration transport including advective and diffusive terms (Greimann et Al., 2008). The application of some of the above dynamical models to study flood propagation (Rahuel et Al., 1989), dam-break flow (Cao et Al., 2004), and antidunes generation (Di Cristo et Al., 2006) demonstrates the relevance of non-equilibrium transport for a thorough analysis of river morphodynamic processes.

Morphological models which naturally account for the dynamics of the solid phase can be derived based on different approaches, commonly employed in various fields of engineering and physics. The group of Université Catholique de Louvain exploited the possibility of predicting river dynamics in presence of rapid transients through a two-layer schematization, in which the upper layer contains clear water and the lower one a water-sediment mixture. Erosion and deposition result from mass exchange between the fixed bed and the transport layer. Following this schematization and assuming equal velocity in the two layers, Fraccarollo and Capart (2002) examined the sudden erosional flow caused by a dam break wave over a loose sediment bed with very promising results. An improvement of the two-layer model was suggested later on by Capart and Young (2002), who considered different velocities in the two layers. The successful application of the latter model to simulate the formation and propagation of a hydraulic jump over a mobile bed is shown in Savary & Zech (2007). The comparison of the computed results with laboratory evidences witnesses the effectiveness of the two-layer approach, even though a hyperbolicity loss of the model may occur (Greco et Al., 2008b; Savary & Zech, 2007b).

Models built up on the two-phase theory have been widely applied in chemical engineering, providing notable insights into the physics of fluidization (Anderson et Al., 1995). In the geophysical context, two-phase formulations have been introduced to study the propagation of debris flows, avalanches and landslides (Iverson, 1997; Pitman & Le, 2005). In open channel hydraulics, this theory has been fruitfully applied to predict the sediment concentration profile in uniform flows, incorporating the effect of particle-particle interaction and particle inertia (Greimann & Holly, 2001)

In the present paper a depth averaged morphodynamical model based on a two-phase formulation is introduced. Mass and momentum conservation principle are separately imposed for both phases, along with the Exner equation to account for bed evolution. Similarly to the two-layer model of Savary and Zech (2007), the present model neither postulates the instantaneous adaptation hypothesis nor employs any *ad hoc* differential equation to mimic sediment transport dynamics.

Model derivation

Sediment transport is herein analysed within the framework of a two-phase approach (Greimann & Holly, 2001; Iverson, 1997; Pitman & Le, 2005). In what follows we will assume that the flow exhibits the distinctive features of bed-load, i.e. particles move in a thin region close to the bed. Within this region, particle motion is intermittent, but at any point the average over a number of particle movements allows to define a macroscopic volume concentration, *C*, which, according to Greimann et Al. (2008), may be equivalently considered as the probability to find a solid particle at a given point in a given time. While flowing, the two phases furthermore interact with the mobile bed, in a local and time-dependent erosion/deposition budget.

The following hypotheses are then introduced:

- Wide rectangular channel with small slope.
- Constant liquid (ρ_l) and solid (ρ_s) densities are assumed. Moreover, sediment is considered as uniform and non-cohesive.
- Flow is gradually varied with hydrostatic pressure distribution in the cross-section, which is assumed to be vertical since the bottom slope is mild.
- Surface concentration is equal to volume concentration, which is assumed constant both in space and time.
- Standing bed is saturated.

Let us assume a control volume (CV) of the fluid – sediments flow of base *dx dy*, *x* and *y* being the horizontal coordinates, the bottom and the free surface (sidewalls effects are neglected due to the wide channel hypothesis), with unitary width. Neglecting higher order terms, the CV measure is $h\,dx\,dy$, with $h = z_{fs} - z_b$, z_{fs} and z_b being the free surface and bottom elevation, respectively. Volume deforms in time due to erosion/deposition budget and flow depth variation. Defining δ_s as the ratio of solid phase volume to the bed surface, the ratio of liquid phase volume to the bed surface, δ_l, is given by $\delta_l = h - \delta_s$.

In the absence of any inflow/outflow from sidewalls and free-surface, the mass conservation requirement for the liquid phase reads:

$$\frac{\partial \delta_l}{\partial t} + \frac{\partial U_l \delta_l}{\partial x} + \frac{\partial V_l \delta_l}{\partial y} + p\frac{\partial z_b}{\partial t} = 0 \qquad (1)$$

where $U_l \delta_l \rho_l$ represents the water mass discharge, U_l being the phase-averaged water velocity in the x direction, V_l the same in the *y* direction and *p* is the bed porosity. The last term in the LHS accounts for the water entering (leaving) the flow due to the erosion (deposition) of the saturated bed. In what follows subscripts *l* and *s* will be used to denote quantities pertaining to liquid and solid phases, respectively.

Similarly, the mass conservation equation for the solid phase reads:

$$\frac{\partial \delta_s}{\partial t} + \frac{\partial U_s \delta_s}{\partial x} + \frac{\partial V_s \delta_s}{\partial y} + (1-p)\frac{\partial z_b}{\partial t} = 0 \qquad (2)$$

in which $\rho_s U_s \delta_s$ is the solid mass discharge, U_s being the phase-averaged solid velocity in the x direction and V_s the same in the *y* direction.

Moreover, the temporal variation of bottom elevation has to satisfy the following constraint:

$$\frac{\partial z_b}{\partial t} = -e_b \qquad (3)$$

Where e_b denotes the bottom erosion/deposition rate.

The projection of momentum balance for the considered CV onto the *x* and *y* directions for each phase reads:

$$\frac{\partial U_l \delta_l}{\partial t} + \frac{\partial}{\partial x}\left(U_l^2 \delta_l + g\frac{(\delta_l+\delta_s)^2}{2}\right) + \frac{\partial}{\partial y}(U_l V_l \delta_l) + g(\delta_l+\delta_s)\frac{\partial z_b}{\partial x} + S_{l,x} = 0 \qquad (4)$$

$$\frac{\partial V_l \delta_l}{\partial t} + \frac{\partial}{\partial x}(U_l V_l \delta_l) + \frac{\partial}{\partial y}\left(V_l^2 \delta_l + g\frac{(\delta_l+\delta_s)^2}{2}\right) + g(\delta_l+\delta_s)\frac{\partial z_b}{\partial y} + S_{l,y} = 0 \qquad (5)$$

$$\frac{\partial U_s\delta_s}{\partial t}+\frac{\partial}{\partial x}\left(U_s^2\delta_s+g\frac{\Delta}{\Delta+1}\frac{\delta_s^{\,2}}{2C}\right)+\frac{\partial}{\partial y}(U_sV_s\delta_s)+g\delta_s\frac{\Delta}{\Delta+1}\frac{\partial z_b}{\partial x}+S_{s,x}=0 \qquad (6)$$

$$\frac{\partial V_s\delta_s}{\partial t}+\frac{\partial}{\partial x}(U_sV_s\delta_s)+\frac{\partial}{\partial y}\left(V_s^2\delta_s+g\frac{\Delta}{\Delta+1}\frac{\delta_s^{\,2}}{2C}\right)+g\delta_s\frac{\Delta}{\Delta+1}\frac{\partial z_b}{\partial y}+S_{s,x}=0 \qquad (7)$$

with:

$$\mathbf{S}_l=\frac{\boldsymbol{\tau}_0-\boldsymbol{\tau}_{b,s}}{\rho_l}+\frac{\mathbf{D}}{\rho_l}=\frac{|\mathbf{U}_l|}{C_h^2}\mathbf{U}_l-\mu_d g\delta_s\frac{(\rho_s-\rho_l)}{\rho_l}\frac{\mathbf{U}_s}{|\mathbf{U}_s|}+C_D\frac{\delta_s}{d}(\mathbf{U}_l-\mathbf{U}_s)|\mathbf{U}_l-\mathbf{U}_s| \qquad (8)$$

$$\mathbf{S}_s=\frac{\boldsymbol{\tau}_{b,s}}{\rho_s}-\frac{\mathbf{D}}{\rho_s}=\mu_d g\delta_s\frac{(\rho_s-\rho_l)}{\rho_s}\frac{\mathbf{U}_s}{|\mathbf{U}_s|}-\frac{\rho_l}{\rho_s}C_D\frac{\delta_s}{d}(\mathbf{U}_l-\mathbf{U}_s)|\mathbf{U}_l-\mathbf{U}_s| \qquad (9)$$

Once the closure relations for $\boldsymbol{\tau}_{b,l}$, $\boldsymbol{\tau}_{b,s}$, D and e_b are specified, the system of equations (1) - (7), allows to compute spatial and temporal evolution of the seven unknowns U_l, V_l, U_s, V_s, δ_l, δ_s, and z_b.

Closure relations

The evaluation of the bed shear stresses acting on the liquid and solid phases, $\boldsymbol{\tau}_{b,l}$ and $\boldsymbol{\tau}_{b,s}$, should account for the physical interaction between the two phases. As described by Seminara et Al. (2002), drag transfers momentum from the liquid to the solid phase, with a twofold effect: liquid loses momentum in favors of solid, so that the shear stress exerted by the fluid at the bottom is smaller than in the absence of sediment transport; the solid phase further transfers the received momentum through repeated collisions with the bottom surface - giving rise to a solid phase shear stress - and with other particles. Seminara et Al. (2002) described this complex interplay through a depth-averaged two-phase momentum balance of the transport layer under uniform flow conditions in presence of bed-load. In the limit of a nearly horizontal bed and neglecting the effect of interparticle collisions, the bottom fluid shear stress that would act in the absence of solid phase is found to be partitioned between the actual fluid shear stress and the stress due to the solid phase. The partition proposed by Seminara et al. (2002) is herein considered to evaluate the stress terms needed for the model closure. Indeed, $\boldsymbol{\tau}_{b,l}$ is computed as the difference between the fluid shear stress that would prevail at the bed in the absence of a transport layer $(\boldsymbol{\tau}_0)$ and the solid shear stress $(\boldsymbol{\tau}_{b,s})$. Following Seminara et al. (2002), the former is evaluated by means of Chezy uniform flow formula, while the latter should account for both frictional and collisional stresses. The frictional contribution $(\boldsymbol{\tau}_{\mu,s})$ may be expressed through Mohr-Coulomb law while the collisional one $(\boldsymbol{\tau}_{c,s})$, based on the findings of Bagnold (1954), may be assumed to scale with the square of the particle average velocity. Since the contribution of collisional stress is expected to be significant only whenever sediment transport occurs as sheet-flow (Gao, 2008), in what follows it has been neglected. Moreover, numerical simulations (results not shown) have confirmed that in the conditions herein investigated, the collisional term is negligible. Therefore, the expressions of tangential stresses on the two phases are:

$$\boldsymbol{\tau}_{b,l}=\boldsymbol{\tau}_0-\boldsymbol{\tau}_{b,s}=\rho_l\frac{|\boldsymbol{U}_l|}{C_h^2}\boldsymbol{U}_l-\boldsymbol{\tau}_{b,s} \qquad (10)$$

$$\boldsymbol{\tau}_{b,s}=\boldsymbol{\tau}_{\mu,s}+\boldsymbol{\tau}_{c,s}\cong\mu_d g\delta_s(\rho_s-\rho_l)\frac{\boldsymbol{U}_s}{|\boldsymbol{U}_s|} \qquad (11)$$

where d is the sediment diameter and μ_d is the friction coefficient in dynamic conditions. The dimensionless Chezy coefficient (i.e. the ratio of the traditional Chezy coefficient to the square of gravitational acceleration) has been denoted with C_h.

Assuming that momentum exchanged by the drag of liquid over particles is uniformly distributed wherever both phases exist, the $\boldsymbol{D}$ term may be expressed as the drag acting on a single particle times the mean number of particles in the control volume:

$$\boldsymbol{D}=\rho_l C_D\frac{\delta_s}{d}(\boldsymbol{U}_l-\boldsymbol{U}_s)|\boldsymbol{U}_l-\boldsymbol{U}_s| \qquad (12)$$

The evaluation of drag coefficient, C_D, can be pursued in uniform condition of flow and in the limit of negligible bottom slope. Indeed in these hypotheses, computing the solid average velocity through the Fernandez-Luque and van Beek (1976) relation, the following the expression for C_D may be obtained:

$$C_D=\frac{\mu_d\sqrt{gd\Delta}}{\left[(C_h-k')\sqrt{\frac{|\boldsymbol{\tau}_0|}{\rho_l}}-k''\sqrt{\frac{|\boldsymbol{\tau}_{c0}|}{\rho_l}}\right]^2} \qquad (13)$$

in which k' and k'' are two dimensionless coefficients ($k'=9.2$ and $k''=0.7$, see Fernandez-Luque and van Beek, 1976) and $|\boldsymbol{\tau}_{c0}|$ represents the value of $|\boldsymbol{\tau}_0|$ in the threshold condition for incipient particle motion. Equation (13) has been employed also in non-uniform conditions and it has been applied locally and instantaneously to evaluate the drag coefficient. In applying (13) the threshold value has been assumed as $|\boldsymbol{\tau}_{c0}|=0.047\rho_l gd\Delta$ (Meyer-Peter and Muller, 1948).

The expression of the entrainment/deposition function e_b is required as a further closure for the present model. Several different formulas, based on theoretical analysis and/or experiments carried out under steady equilibrium flows, can be found in the literature for both entrainment and deposition fluxes (see for instance: Van Rijn 1984; Fraccarollo and Capart, 2002, Seminara et Al., 2002; Parker et Al., 2003). In the following, the net entrainment from the bed is computed as the difference between the erosion and deposition flux predicted by the formulas provided in Parker et al. (2003), which have been demonstrated to correctly reproduce the experimental findings of Fernandez Luque and van Beek (1976):

$$e_b = E - D = 0.02\sqrt{gd\Delta}\left[\left(\frac{|\boldsymbol{\tau}_0| - |\boldsymbol{\tau}_{c0}|}{\rho_l g d \Delta}\right)^{3/2} - \left(\frac{1}{0.83}\frac{\delta_s}{d}\right)^{3/2}\right] \quad (14)$$

It is worth of remark that, once the dynamical friction coefficient of the sediment is known, similarly to the clear-water case (i.e. Saint Venant equations), the only parameter that need to be assigned for the application of the model is the dimensionless Chezy coefficient.

The equations describing the proposed model constitute an hyperbolic PDEs system, which may be solved with any of the numerical schemes commonly employed for Saint-Venant Equations. The Finite Volume solver FIVFLOOD (Leopardi et Al., 2002) has been adapted to solve the PDEs of the two-phase model.

Numerical Simulation

In order to demonstrate the effectiveness of the proposed model a 2DH test is presented. The application consists in a dam-break flow over a movable bed with a sudden enlargement (Palumbo et Al., 2008). The tests were performed in a 6 m long flume, with an asymmetrical sudden increase on the channel width from 0.25 m to 0.5 m on the left side, 1 m downstream of the gate (Figure 1). The breaking of the dam is simulated by the rapid (about 0.1 s) downward movement of a thin gate at the middle of the flume. The sediment used is uniform sand with a median diameter d_{50} of 1.72 mm, static friction angle μ_0 = 30°, relative density Δ=1.63, deposited with porosity p = 0.61. Initial conditions consist of a 0.1 m layer of fully saturated and compacted sand over the whole flume, and an initial layer of 0.25 m water upstream of the gate (Figure 1).

Temporal evolution of the free surface elevation was recorded by ultrasonic gauges in 8 probes, while the final bed topography was measured in 9 cross sections in the wider channel using a photographic technique (see Palumbo et Al. (2008) for details). From the above dataset, three gauges (denoted as P1, P2 and P3) and two cross sections (named A and B, respectively), positioned as indicated in Figure 1, will be considered herein for comparison with the model predictions.

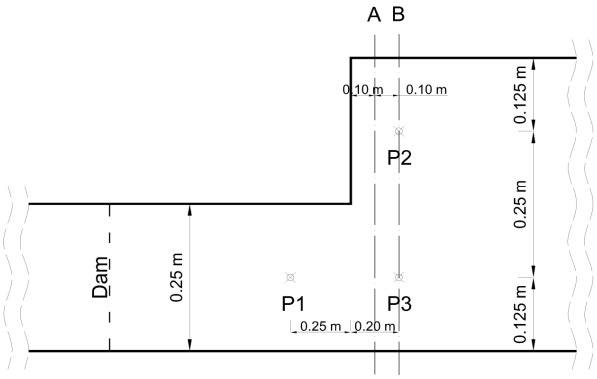

Figure 1: Experimental set-up.

A space grid with square elements $\Delta x = \Delta y$ = 0.0125 m was employed in the simulations, along with a times step Δt =$2\cdot10^{-4}$ s. The value of the dimensionless coefficient in the Chezy formula was set equal to the previous cases based again on the similarity of the sediments employed. In order to guarantee a realistic simulation of the complete emptying of the flume, boundary conditions were assigned correspondently to the experimental setting, namely a fixed-wall was considered at the upstream boundary and a subcritical/supercritical free-flow for both water and sediment flow at the channel outlet.

The simulated geomorphic transient develops with the distinctive features observed by the experimenters: once the dam break wave has reached the downstream end of the narrow channel, flow curves left-wise and moves towards the sidewall. Wall reflection induces the appearance of an oblique bore, which propagates downstream and finally disappears as the flume empties.

The evolution of the loose bed is characterised by two morphological features which are closely related to the above hydrodynamics. Streamlines curvature close to the inner corner causes the appearance of a deep scour, while the sudden rise of the water level downstream the bore causes an elongated deposit in the left portion of the wide channel. Both features are reproduced in the simulations, and are clearly noticeable in the snapshot of the results at t = 4 s depicted in Figure 2. The flow field is represented by two families (bold and thin) of streamlines, representing water and sediment velocities, respectively. Bottom configuration is represented by continuous and dashed contours for deposition and scouring zones, respectively.

As it can be seen, in the zone close to the inner corner and in the adjacent flow separation zone, the direction of the solid transport differs significantly from that of the liquid phase, witnessing the different response of the two phases to bottom topography, attrition and drag. Curvature of

velocity field is more evident for water than for sediment, as it could be expected due to their different inertia. Moreover, the strong recirculation zone behind the enlargement is not significantly affected by sediment transport.

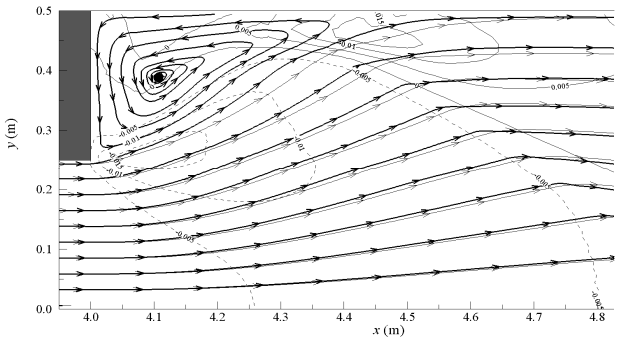

Figure 2: Streamlines of liquid and solid phase, superposed to bottom topography, t = 4 s.

In order to provide a quantitative assessment of the performance of the two-phase model, in Figures 3a-c the comparison between measured and computed free surface elevation for the gauges P1, P2 and P3 is represented. Moreover, in Figure 4a-b the final bottom topography is shown. In both figures, the numerical results of the two-layer model of Soares-Frazão and Zech (2010) are superposed.

The measured water heights are reasonably reproduced for all the probes P1-P3 (see Figure 3). Average absolute deviation between predicted and observed free surface elevation is less than 10%, with a correlation coefficient always above 0.85 between measured and computed values.

Numerical results exhibit a qualitative agreement with the measures, since the deposit location is predicted to be more downstream than observed. (Figures 4a-b). On the other hand, the shape of the most scoured zone is well reproduced (section A), along with the estimated maximum depth, which agrees with the observed one within 13% accuracy, whereas a systematic underprediction of deposition is observed in the considered cross sections. Figures 3 and 4 show that the performance of the two-phase and two-layer models is similar, with a common underprediction of deposition near the side wall.

The latter discrepancy has been ascribed by Soares-Frazão and Zech (2010) to the presence of three-dimensional effects occurring close to the wall, which cannot be accounted for by shallow water models.

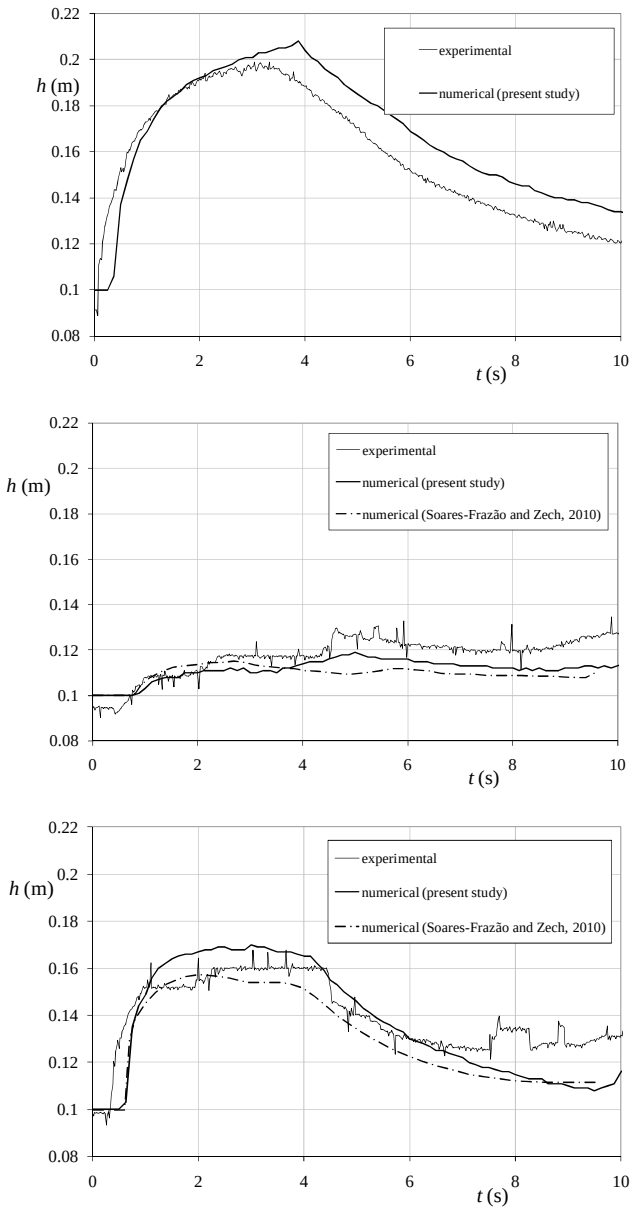

Figure 3: Time history of free surface elevation. From top to bottom: probe P1, probe P2, probe P3.

Conclusions

In the paper a shallow water model for the analysis of fast geomorphic transients occurring in the context of river morphodynamics has been presented. The model is based on a two-phase formulation and it has been derived from mass and momentum conservation principles applied to sediment and water.

Comparison with literature experimental data shows the capabilities of the two-phase approach in reproducing fast morphodynamic transients. Furthermore, the present model has been shown to perform similarly to other well assessed morphodynamic models, without requiring any explicit lag relation and preserving the hyperbolic character. Future

developments will consider additional two-dimensional test cases to further validate the model.

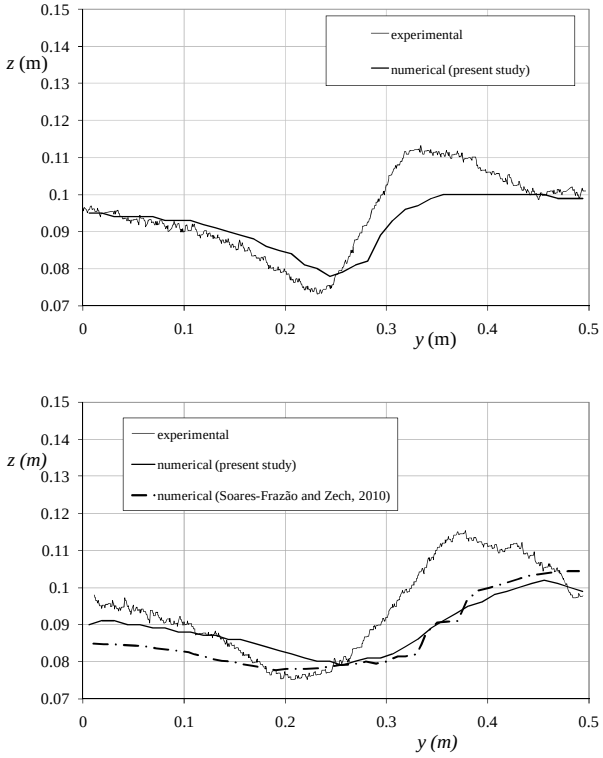

Figure 4: Final bottom topography. a) cross section A; b) cross section B.

References

Anderson K., Sundaresan S. and Jackson R., Instabilities and the formation of bubbles in fluidized beds. *J. Fluid Mech.* 303, 1995, 327–366.

Armanini A. and Di Silvio G., A one-dimensional model for the transport of a sediment mixture in non-equilibrium conditions. *J. Hydraul. Res*, 26(3), 1988, 275–292.

Bagnold R.A., Experiments on a gravity-free dispersion of large solid spheres in a Newtonian fluid under shear. *P. Roy. Soc. A-Math. Phy.*, 1954, 225, 49–63.

Benoist G., Les ètudes d'ondes de submersion des grand barrages d'EDF. *La Houille Blanche*, 1, 1989, 43–54 (in French).

Brooks G.R. and Lawrence D.E., The drainage of the Lake Ha! Ha! reservoir and downstream impacts along Ha! Ha! River, Saguenay area, Quebec, Canada. *Geomorphology*, 28, 1999, 141–168.

Cao Z. and Carling P.A., Mathematical modelling of alluvial rivers: reality and myth. Part 1: general overview. *Marit. Eng.*, 154(3), 2002, 207–219.

Cao Z., Pender G., Wallis S. and Carling, P., Computational dam-break hydraulics over erodible sediment bed. *J. Hydraul. Eng.-ASCE*, 130(7), 2004, 689–703.

Capart H. and Young D., Two-layer shallow water computations of torrential geomorphic flows. *Proc. River Flow 2002*, 2002, 1003–1012.

Di Cristo C., Leopardi A. and Greco M., A bed load transport model for non-uniform flows. *Proc. of River Flow 2002*, 2002, 859–864.

Fernandez Luque R. and Van Beek R., Erosion and Transport of Bed-Load Sediment, *Journal of Hydraulic Research*, 14(2), 1997, 127–144.

Fraccarollo L. and Capart H., Riemann wave description of erosional dam-break flows. *J. Fluid Mech.*, 461, 2002, 183–228.

Gao, P., Transition between Two Bed-Load Transport Regimes: Saltation and Sheet Flow. *Journal of Hydraulic Engineering*., 134(3), 2008, 340–349.

Graf W. H. (with Altinakar M.), Fluvial Hydraulics: Flow and Transport Processes in Channels of Simple Geometry. *John Wiley & Sons, 1998.*

Greco M., Iervolino M. and Leopardi A., Discussion on "Divergence Form for Bed Slope Source Term in Shallow Water Equations. *J. Hydraul. Eng.-ASCE*, 134(5), 2008, 676–678.

Greco M., Iervolino M. and Vacca A., Discussion on "Boundary conditions in a two-layer geomorphological model: application to a hydraulic jump over a mobile bed." by Savary C. and Zech Y. (2007). *J. Hydraul. Res.*, 46(6), 2008, 856–858.

Greimann B. and Holly F., Two-Phase Flow Analysis of Concentration Profiles. *J. Hydraul. Eng.-ASCE*, 127(9), 2001, 753–762.

Greimann B., Lai Y. and Huang J., Two-dimensional total sediment load model equations *J. Hydraul. Eng.-ASCE*, 134(8), 2008, 1142–1146.

Hu P. and Cao Z., Fully coupled mathematical modeling of turbidity currents over erodiblebed. *Adv. Water Resour.*, 32, 2009, 1–15.

Iverson R.M., The physics of debris flows. *Rev. Geophys.*, 35, 1997, 245–296.

Leopardi A., Oliveri E. and Greco M., Two-Dimensional Modeling of Floods to Map Risk Prone Areas. *J. Water Res. Pl.-ASCE*, 128, 2002, 168–178.

Meyer-Peter E. and Muller R., Formulas for bed-load transport. *Proc. of Intern. Assoc. Hydr. Res., 2d Meeting, Stockholm*, 1948.

Palumbo A., Soares-Frazão S., Goutiere L., Pianese D., Zech Y., Dam-break flow on mobile bed in a channel with a sudden enlargement. *Proc. of Riverflow 2008*, 2008, 645–54.

Parker G., Sediment inertia as cause of river antidunes. *J. Hydraul. Div.-ASCE*, HY2, 1975, 211–221.

Parker, G., Seminara G., and Solari L., Bed load at low Shields stress on arbitrarily sloping beds: alternative entrainment formulation. *Water Resour. Res.*, 39(7), 2003, 1183–1194, DOI: 10.1029/2001WR001253.

Pitman E.B. and Le L., A two-fluid model for avalanche and debris flows. *Phil. Trans. R. Soc. A*, 363, 2005, 1573–1601.

Savary C. and Zech Y., Boundary conditions in a two-layer geomorphological model: application to a hydraulic jump over a mobile bed. *J. Hydraul. Res.*, 45(3), 2007, 316–332.

Savary C. and Zech Y., Closure on "Boundary conditions in a two-layer geomorphological model: application to a hydraulic jump over a mobile bed." by Savary C. and Zech Y. (2007). *J. Hydraul. Res.*, 46(6), 2008, 858–860.

Seminara G., Solari L. and Parker G., Bedload on arbitrary sloping beds. Part 1: Failure of the Bagnold hypothesis. *Water Resour. Res.*, 38(11), 2002, 1249–1271.

Simpson G. and Castelltort S., Coupled model of surface water flow, sediment transport and morphological evolution. *Computat. Geosci.*, 32, 2006, 1600–1614.

Soares-Frazão S. and Zech Y., HLLC scheme with novel wave-speed estimators appropriate for two-dimensional shallow-water flow on erodible bed. *Int. J. Numer. Meth. Fluids*, 2010, DOI:10.1002/fld.2300

Van Rijn L.C., Sediment Pick-Up Functions. *J. Hydraul. Eng.-ASCE*, 110(10), 1984, 1494–1502.

Wu, W., *Computational River Dynamics*. Routeledge. Taylor & Francis Group, 2007.